Arbitrage with Power Factor Correction using Energy Storage

Md Umar Hashmi[1], Deepjyoti Deka[2], Ana Bušić[1], Lucas Pereira[3], and Scott Backhaus[2]

The importance of reactive power compensation for power factor (PF) correction will significantly increase with the large-scale integration of distributed generation interfaced via inverters producing only active power. In this work, we focus on co-optimizing energy storage for performing energy arbitrage as well as local power factor corrections. The joint optimization problem is non-convex, but can be solved efficiently using a McCormick relaxation along with penalty-based schemes. Using numerical simulations on real data and realistic storage profiles, we show that energy storage can correct PF locally without reducing arbitrage gains. It is observed that active and reactive power control is largely decoupled in nature for performing arbitrage and PF correction (PFC). Furthermore, we consider a stochastic online formulation of the problem with uncertain load, renewable and pricing profiles. We develop a model predictive control based storage control policy using ARMA forecast for the uncertainty. Using numerical simulations we observe that PFC is primarily governed by the size of the converter and therefore, look-ahead in time in the online setting does not affect PFC noticeably. However, arbitrage gains are more sensitive to uncertainty for batteries with faster ramp rates compared to slow ramping batteries.

I. Introduction

With the growth of distributed generation (DG) and large-scale renewables, the need to understand their effects on power networks has become crucial. While bulk-renewable generators have well defined rules for performance including that for reactive power, distributed generation owned by small residential consumers have been exempted. This is primarily due to lack of measurement infrastructure and installed DG contributing to a small fraction of total generation. However, in recent years, growing incentives and environmental awareness have resulted in a large number of consumers installing distributed generation. Policies such as Net-Energy Metering in California has lead to more than 913,481 California electricity consumers opting for solar installations by the end of 2018[1]. Understanding the effects, both operational and financial, of growth in distributed energy resources (DERs) is essential for Distribution System Operators (DSOs) to ensure reliable operation. Since DERs in current markets are not financially rewarded for providing reactive power support, small inverters connected to them primarily output active power and almost no reactive power [1]. This is also in compliance with IEEE Standard 1547, which specifies that DG shall not actively regulate the voltage at the point of common coupling [2]. As a result, there has been a degradation of the load power factor (PF) [3].

PF denotes the ratio of active power and the apparent power and is measured as $\cos(\phi)$, where ϕ denotes the angle between active and reactive power. An alternate definition for PF commonly used in national and ISO level power norm documents is $\tan(\phi)$ (denoted as tg ϕ). As distribution grids are primarily designed to operate close to unity power factor, a systematic degradation in PF can lead to high current, excessive thermal losses, aggravated voltage profiles [4], and equipment damage. It has been shown that maintaining a high power factor leads to positive environmental effects due to increased grid efficiency [5]. To this end, several regional transmission organizations and system operators have operational rules for PF as stated in Table I, though primarily for large loads. Note that $|\cos(\phi)|$ implies symmetric rules for leading and lagging power factor.

TABLE I: Power Factor Correction Rules

Utility/Country Name	PF Limit
France [6] (for $>$ 252 kVA)	$\lvert \text{tg } \phi \rvert \leq 0.4$
Portugal [7], Uruguay [8]	$\lvert\cos(\phi)\rvert \geq 0.92$
Germany [9] (for solar users $>$3.68 kVA)	$\lvert\cos(\phi)\rvert \geq 0.95$
CAISO: (a) Wind Generators [10]	$\lvert\cos(\phi)\rvert \geq 0.95$
(b) Producers in Dist. Grid [11],[12],[13]	$\lvert\cos(\phi)\rvert \geq 0.9$
(c) Consumers in PG&E [14]	$\lvert\cos(\phi)\rvert \geq 0.85$
PJM: for Wind Generators[10]	$\lvert\cos(\phi)\rvert \geq 0.95$
ERCOT: for all Generators since 2004 [15]	$\lvert\cos(\phi)\rvert \geq 0.95$
FirstEnergy, Ohio [16]	$\lvert\cos(\phi)\rvert \geq 0.85$
Hydro Ottawa, Canada [17]	$\lvert\cos(\phi)\rvert \geq 0.9$

However the PF of residential consumers is also a point of concern. For example, the Smart Islands Energy Systems (SMILE) project, initiated by the European Union in 2017 [18], involves data collection at multiple fronts including consumer smart meters in Madeira, Portugal. As a case study, 15 minute averaged household consumption and solar generation data on 18$^{\text{th}}$ May, 2018 for a representative residential consumer in the island of Madeira, Portugal is depicted in Fig. 1. Note that while PF at night is close to unity, during the day it degrades significantly due to solar output. Thus low load PF may be subjected to norms and penalties [3], [1]. Some household smart meters (Eg. Linky smart meters in France) already have reactive power monitoring capability that can implement PF norms [19]. The LV consumers in Uruguay have electricity bills with three different contracts [8] that include penalties for PF degradation.

A. Literature Review

While additional infrastructure such as capacitor banks [20] have been proposed to improve power factor, we focus our work on using conventional energy storage/battery for performing power factor correction, in addition to other functions like arbitrage [21], [22]. Note that storage devices generate DC power and hence are connected to the grid through a DC/AC converter/inverter that are often over-sized compared to the installed DER facility [23]. Utilizing the storage converter/inverter and power electronics [24] for power factor correction averts additional investment. The overarching goal of this paper is to demonstrate through novel

[1]M.U.H. and A.B are with INRIA, DI ENS, Ecole Normale Supérieure, CNRS, PSL Research University, Paris, France.
[2]D.D. and S.B. are with Los Alamos National Laboratory, USA
[3]L.P. is with Madeira-ITI/ LARSyS and prsma.com, Funchal, Portugal.

[1]https://www.californiadgstats.ca.gov/, January, 2019

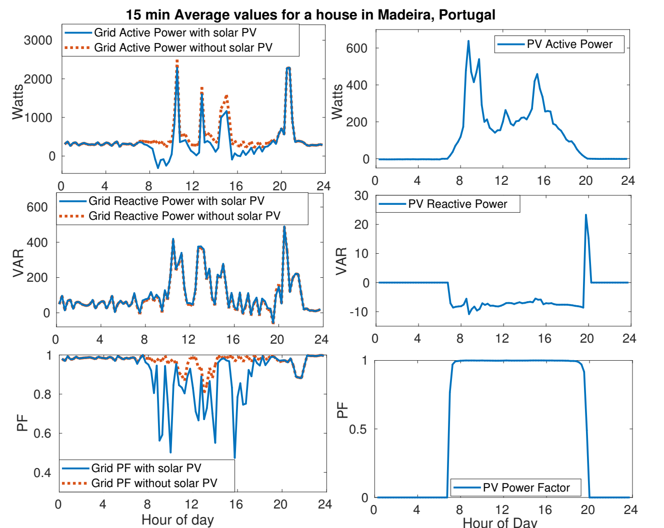

Fig. 1: Variation of active, reactive power and absolute value of power factor for PV and the power seen from the grid

co-optimization formulations that batteries can be used for PFC without any significant effect on arbitrage gains, for a range of price, consumption and PV settings. Note that due to the high cost of storage deployment, researchers have proposed using storage for co-optimization additional goals along with energy arbitrage (temporal shift of active load) for financial feasibility [25]. Inverter reactive power output depends on its control design [26], [27] and can be governed by terminal voltage and/or active power measurements [23], [28]. The authors in [29] use energy storage for maintaining voltages at wind facilities. Similarly, storage devices have been evaluated using power hardware-in-loop for minimizing losses and voltage fluctuations [30]. The authors in [31], [32] co-optimize storage for arbitrage, peak shaving and frequency regulation. Unlike the described prior work, we discuss storage for co-optimization of arbitrage and *power factor correction*. Note that contemporary solar inverters in low voltage operate close to unity power factor (UPF) due to no reactive power obligations and hence are practically ineffective for power factor correction.

B. Contribution

We are interested in using energy storage connected through an inverter for the joint task of arbitrage and PFC. In addition to commercial and residential electricity consumers, the formulation is also of interest for renewable integrators, transmission and distribution operators [33]. The **first** contribution of this work is the development of a non-convex mixed-integer formulation to optimize storage for arbitrage and power factor correction in the presence of DG. While the co-optimization problem is non-convex, we demonstrate three different approximation schemes to solve the problem: (a) McCormick relaxation for original non-convex program, (b) receding horizon arbitrage with real-time PFC, and (c) arbitrage with penalty-based PFC. While the McCormick relaxation and real-time PFC policies routinely achieve the optimal solution, the penalty based approach is able to provide best alternatives in scenarios where no feasible solution satisfying PF limits exists. **Second**, we present a modified penalty-based algorithm that reduces converter usage along with arbitrage and PFC. **Third**, using realistic pricing, net load (consumption + solar) data and battery parameters, we extensively benchmark the achievable ability of storage devices to maintain PF limits without any significant degradation in arbitrage gains. **Fourth**, we consider stochastic extensions of our algorithms for real-time implementation through Model Predictive Control (MPC). We use Auto-Regressive Moving Average (ARMA) processes to model temporally evolving signals in the MPC framework and demonstrate significant benefits from the online algorithms.

The paper is organized in six sections. Section II provides the system description. Section III formulates the co-optimization problem of performing arbitrage and PFC using storage and discusses multiple solution strategies. Section IV presents an online algorithm using ARMA forecasting and MPC in order to mitigate the effect of forecast error. Section V presents the numerical results. Section VI concludes the paper and discusses future directions of research.

II. System Description

The system considered in this work consists of an electricity consumer with inelastic demand, renewable generation (rooftop solar) and energy storage battery. The block diagram of the system considered is shown in Fig. 2. We denote time

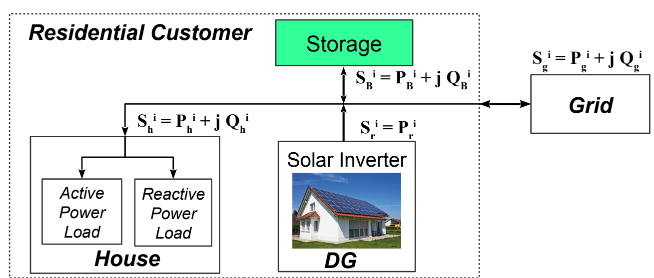

Fig. 2: Residential Load block diagram with DG and storage

instant as a superscript of the variable. The apparent power of the load shown in Fig. 2, at i^{th} time instant is denoted as $S_h^i = P_h^i + jQ_h^i$, where P_h^i and Q_h^i are the active and reactive power consumed. Apparent power of the solar inverter is given as $S_r^i = P_r^i$ where P_r^i is the active power supplied by solar inverter. We assume the solar inverter operates at unity PF. Let us denote the combined load and renewable active and reactive power by $P^i = P_h^i - P_r^i$ and $Q^i = Q_h^i$ respectively. The power factor seen by the grid is the ratio of real power supplied or extracted by the grid over the apparent power seen by the grid. In the absence of storage it is given by

$$\text{pf}_{\text{bc}}^i = P^i / \sqrt{{P^i}^2 + {Q^i}^2}. \tag{1}$$

Observe that PF before correction, pf_{bc}^i, degrades as P_r^i and Q_h^i increases in magnitude. Next we discuss the battery model considered and its effect on PF.

Battery Model: The storage/battery converter can supply active and reactive power. The apparent power output of energy storage (connected through a converter which is an inverter or a rectifier) is given as $S_B^i = P_B^i + jQ_B^i$, where

P_B^i, Q_B^i denote active and reactive power outputs respectively. We consider operation over a total duration T, with operations divided into N steps indexed by $\{1, ..., N\}$. The duration of each step is denoted as h. Hence, $T = hN$. We denote the change in the energy level of the battery at i^{th} instant by x^i; $x^i > 0$ implies charging and $x^i < 0$ implies discharging. x^i/h denotes the corresponding storage ramp rate with $\delta_{\min} \leq 0$ and $\delta_{\max} \geq 0$ as the minimum and maximum ramp rates (kW) respectively. Let the efficiency of charging and discharging of battery be denoted by $\eta_{ch}, \eta_{dis} \in (0, 1]$, respectively. The storage active power P_B^i for the i^{th} instant is related to battery energy as $P_B^i = \frac{[x^i]^+}{h\eta_{ch}} - \frac{[x^i]^- \eta_{dis}}{h}$. The active power ramp rate constraint follows as

$$P_B^i \in [P_B^{\min}, P_B^{\max}] \ \text{ with } P_B^{\min}=\delta_{\min}\eta_{dis},\ P_B^{\max}=\frac{\delta_{\max}}{\eta_{ch}}, \quad (2)$$

Though the battery charge level is not affected by the reactive power output Q_B^i of the connected inverter, the amount of active power supplied or consumed is dependent upon it due to the line current limitations [34]. The converter rating is given by the maximum apparent power supplied/consumed, denoted as $S_B^{\max}$ which bounds the instantaneous apparent power S_B^i

$$(S_B^{\max})^2 \geq (S_B^i)^2 = (P_B^i)^2 + (Q_B^i)^2, \quad (3)$$

Let b^i denote the energy stored in the battery at the i^{th} step with $b^i = b^{i-1} + x^i$. To keep the charge in the battery within prescribed limits, the battery capacity constraint is imposed

$$b^i \in [b_{\min}, b_{\max}], \quad (4)$$

where $b_{\min} = SoC_{\min}B_{rated}$ and $b_{\max} = SoC_{\max}B_{rated}$. B_{rated} is the rated capacity and $SoC_{\min}$ and $SoC_{\max}$ are the minimum and maximum level of state of charge respectively.

Energy Arbitrage: The primary use of the storage device considered here is for 'Energy arbitrage' which refers to buying electricity when price is low and selling it when price is high, and in effect making a profit. In this work we assume that buying and selling prices of electricity at each instant i are the same and denote it by p_{elec}^i. Under this assumption, the arbitrage gains depend on the varying electricity price but not on the inflexible load. As monetary benefits from arbitrage is *based only on* active power, the operator seeks to minimize the following problem:

$$(P_{arb}) \quad \min \sum_{i=1}^{N} p_{elec}^i P_B^i, \quad \text{subject to: Eqs. 2, 4}$$

We refer the readers to [35] for additional details.

Power Factor Correction: Note the power factor formulation in Eq. 1. In the presence of storage, it takes the form

$$pf_c^i = P_T^i / \sqrt{(P_T^i)^2 + (Q_T^i)^2}, \quad (5)$$

where total active power and reactive powers are given by

$$P_T^i = P^i + P_B^i, \quad Q_T^i = Q^i + Q_B^i. \quad (6)$$

It is clear that storage operations can negatively or positively affect the load PF. To ensure that the PF is within the permissible limits,

$$-k \leq \frac{Q_T^i}{|P_T^i|} \leq k, \quad \text{where } k = \tan(\theta_{\min}). \quad (7)$$

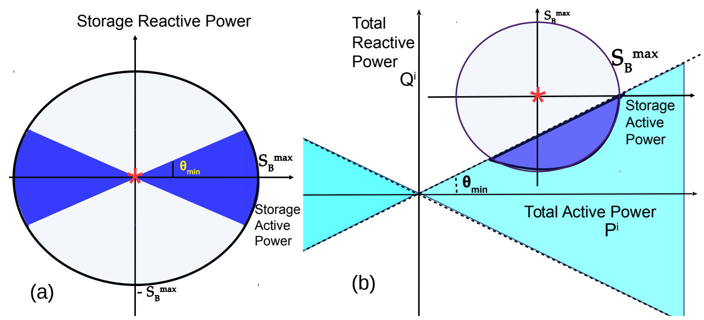

Fig. 3: (a) Shows the feasible region of storage in absence of load and DG. The active power out of storage converter, $P_B^i \in [-P_B^{\max}, P_B^{\max}]$, and reactive power output ranges as $Q_B^i \in [-S_B^{\max}, S_B^{\max}]$. The utility sets the power factor limit $\text{pf}_{\min}$, which corresponds power angle $\theta_{\min} = \cos^{-1}(\text{pf}_{\min})$. The deep blue shaded region shows the feasible region of converter operation where output power factor lies within permissible limits of PF. In this plot we assume $P_B^{\max} \geq S_B^{\max}$. (b) Shows the feasible region in presence of load and DG. The active and reactive power without storage is shown with red asterisk.

We assume that the limits in Eq. 7 are identical for both leading and lagging PF. Note that the feasible region for the PF constraint as shown in Fig. 3(a) is not convex. In the next section we will formulate a non-convex storage optimization problem and discuss solution strategies.

III. Arbitrage and PFC with Storage

We formulate the co-optimization problem for performing arbitrage and correcting power factor considering active (P_B^i) and reactive power (Q_B^i) output from storage connected via an inverter. Following the discussion in the preceding section, the objective function is given as

$$(P_{org}) \quad \min_{P_B^i, Q_B^i} \sum_{i=1}^{N} p_{elec}^i P_B^i, \quad \text{subject to, Eqs. 2, 3, 4, 6, 7.}$$

Eq. 7 is non-convex but consists of two disjoint convex sets if the active power in the denominator is sign-restricted. Approaches to solve it are discussed next.

A. McCormick Relaxation based approach

McCormick envelopes are a type of relaxation used in bi-linear nonlinear programming problems as solving non-convex problems are difficult. The McCormick envelope guarantees convexity but keeps the bounds sufficiently tight [36]. To use it , we reformulate the non-convex PF constraint (7) in (P_{org}) to a bi-linear constraint by introducing binary variables z as $|P_T^i| = (2z-1)P_T^i$. Let $y = zP_T^i$ denote the bi-linear variable. We then have

$$(2z-1)P_T^i \geq 0 \implies 2y - P_T^i \geq 0.$$

The McCormick relaxation [37] for the bi-linear term is represented as follows

$$y \geq z_{lb}P_T^i + P_{lb}^i z - z_{lb}P_{lb}^i, \quad y \geq z_{ub}P_T^i + P_{ub}^i z - z_{ub}P_{ub}^i,$$
$$y \leq z_{lb}P_T^i + P_{ub}^i z - z_{lb}P_{ub}^i, \quad y \leq z_{ub}P_T^i + P_{lb}^i z - z_{ub}P_{lb}^i.$$

where z_{lb} (z_{ub}) and P^i_{lb} (P^i_{lb}) are the lower (upper) bounds for z and P^i_T respectively. As $z_{lb} = 0$ and $z_{ub} = 1$, the above constraints simplify to

$$y \geq P^i_{lb} z, \quad y \geq P^i_T + P^i_{ub} z - P^i_{ub}$$
$$y \leq P^i_{ub} z, \quad y \leq P^i_T + P^i_{lb} z - P^i_{lb}.$$

As mentioned in [38], this McCormick relaxation is exact as one of the variables in the bi-linear term is a binary variable. After simplification, we get the following mixed-integer convex problem (P_{mr}) for (P_{org}).

$$(P_{mr}) \quad \min_{P_B, Q_B} \quad \sum_{i=1}^{N} p^i_{elec} P^i_B$$
$$\text{subject to, Eqs. 2, 3, 4, 6}$$
$$\text{PF constraint: } -2ky + kP^i_T - Q^i_T \leq 0,$$
$$-2ky + kP^i_T + Q^i_T \leq 0,$$
$$\text{Binary variable: } z \in \{0,1\}, \quad 2y - P^i_T \geq 0,$$
$$\text{McCormick constraint: } \quad y \geq P^i_{lb} z, \quad y \leq P^i_{ub} z,$$
$$y \geq P^i_T + P^i_{ub} z - P^i_{ub}, \quad y \leq P^i_T + P^i_{lb} z - P^i_{lb}.$$

Here $P^i_{lb} = P^i + P^{\min}_B$ is the lower bound of total active power, and $P^i_{ub} = P^i + P^{\max}_B$ is the upper bound. Problem (P_{mr}) involving mixed-integer linear constraints can be solved by off the shelf solvers like Gurobi or Mosek that can be called by CVX [39]. Note that both (P_{org}, P_{mr}) consider arbitrage and PFC at equal footing for all time instances. To study the impact of PFC on arbitrage gains, we propose an approach next where PF of the current instance alone is considered while making optimal arbitrage decisions.

B. Receding horizon arbitrage with sequential PFC

We consider a receding horizon approach (P_{rh}) that solves two disjoint optimization problems, denoted as (P_{sub_1}) and (P_{sub_2}) below, for each time instant j and selects the solution with higher gains and feasibility.

$$(P_{sub_1}) \quad \min_{P_B, Q_B} \quad \sum_{i=j}^{N} p^i_{elec} P^i_B$$
$$\text{subject to, Eqs. 2, 3, 4, 6}$$
$$-kP^j_T \leq Q^j_T \leq kP^j_T, \quad P^j_T \geq 0,$$

and the second sub problem is given as

$$(P_{sub_2}) \quad \min_{P_B, Q_B} \quad \sum_{i=j}^{N} p^i_{elec} P^i_B$$
$$\text{subject to, Eq. 2, 3, 4, 6}$$
$$-kP^j_T \geq Q^j_T \geq kP^j_T, \quad P^j_T < 0.$$

Note that both (P_{sub_1}),(P_{sub_2}) are convex and solve a cumulative arbitrage gains problem, but with PFC restricted to the current time-instant j only (no look-ahead PFC). The sub-problems only differ in the sign of the current total active power P^j_T. The feasible sub-problem with higher gains sets the storage actions for the current instant j, $(P^j_B)^*$ and $(Q^j_B)^*$. The approach then moves to the next instance $j+1$.

Formulations (P_{org}), (P_{mr}), (P_{rh}) model the PF constraints as hard constraints and ensure their feasibility at every operational point. However, PF violations may be unavoidable and no feasible solution may exist. This may be due to converter limitations as well as storage constraints with regard to capacity and ramping. In such cases, we propose an alternate approach where we correct PF as best as possible.

C. Arbitrage with penalty based PFC

We redefine problem (P_{org}) using a penalty function $\theta(i)$ for the power factor. The objective of the new formulation (P_{plt}) is given by

$$\min_{P_B, Q_B} \quad \sum_{i=1}^{N} \left\{ p^i_{elec} P^i_B + \theta(i) \right\}, \tag{8}$$

where we define penalty function $\theta(i)$ as

$$\theta(i) = \lambda \max(0, |Q^i_T| - k|P^i_T|). \tag{9}$$

Here λ represents the constant associated with the linear cost of violating the PF. The shape of penalty function is shown in Fig. 4. The second term in Eq. 9 represents the amount of

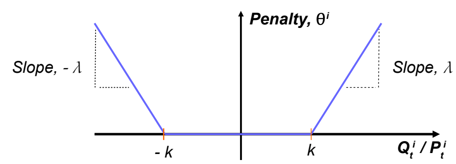

Fig. 4: Penalty function with power factor variation

PF deviation from preset thresholds. This term will be equal to zero for cases where PF is within permissible limits. The max term can be modelled as two constraints

$$\theta(i) \geq 0, \quad \theta(i) \geq \lambda(|Q^i_T| - k|P^i_T|) \tag{10}$$

where absolute value function $|x|$ can further be represented as $(2z-1)x \geq 0$ with binary variable $z \in \{0,1\}$. Eq. 10 can now be reformulated as

$$\begin{aligned} &\theta(i) \geq 0, \quad \theta(i) \geq \lambda(2y^i_1 - Q^i_T - 2ky^i_2 + kP^i_T). \\ &2y^i_1 - Q^i_T \geq 0, \quad 2y^i_2 - P^i_T \geq 0 \end{aligned} \tag{11}$$

Here y^i_1 and y^i_2 denote bi-linear variables

$$y^i_1 = z^i_1 Q^i_T, \quad y^i_2 = z^i_2 P^i_T \tag{12}$$

with binary variables z^i_1 and z^i_2. As before, we use McCormick relaxation to convert the bi-linear terms in Eq. 12 to mixed-integer linear constraints

$$\begin{aligned} y^i_1 &\geq Q^i_{lb} z^i_1, \quad y^i_1 \geq Q^i_T + Q^i_{ub} z^i_1 - Q^i_{ub} \\ y^i_1 &\leq Q^i_{ub} z^i_1, \quad y^i_1 \leq Q^i_T + Q^i_{lb} z^i_1 - Q^i_{lb} \\ y^i_2 &\geq P^i_{lb} z^i_2, \quad y^i_2 \geq P^i_T + P^i_{ub} z^i_2 - P^i_{ub} \\ y^i_2 &\leq P^i_{ub} z^i_2, \quad y^i_2 \leq P^i_T + P^i_{lb} z^i_2 - P^i_{lb}. \end{aligned} \tag{13}$$

In these equations, $Q^i_{lb} = Q^i - S^{\max}_B$ and $Q^i_{ub} = Q^i + S^{\max}_B$ denote the lower and upper bounds respectively for total reactive power.

To summarize, the optimization problem for performing arbitrage and penalization PF violations and its associated constraints are given as

$$(P_{plt}) \quad \min_{P_B, Q_B} \quad \sum_{i=1}^{N} \left\{ p_{elec}^{i} P_B^{i} + \theta(i) \right\}$$
$$\text{subject to, Eq. 2, 3, 4, 6, 11, 13.}$$

Note that while our approach uses linear costs for PF violations, the methodology can be extended to nonlinear penalties in a similar way.

D. Minimizing converter usage with arbitrage and PFC

Power electronic converters degrade with usage [40]. It is in the best interest of energy storage owners to minimize the converter operation, measured in apparent power output, to expand their lifetime. In order to emulate this we propose addition of converter usage component in the objective function of the new optimization problem (P_{plt}^{conv}). The new objective function consists of three components: (a) increase arbitrage gains, (b) reduce PF penalty and (c) reduce converter usage and is given as

$$\min_{P_B, Q_B} \sum_{i=1}^{N} \left\{ p_{elec}^{i} P_B^{i} + \theta(i) + \beta \left((P_B^i)^2 + (Q_B^i)^2 \right) \right\}$$

The optimization problem (P_{plt}^{conv}) is subject to the same constraints as (P_{plt}).

IV. Modeling Uncertainty

The previous section discussed arbitrage and PFC under complete knowledge of future net loads and prices. In this section, we consider the setting where future values may be unknown. To that end, we first develop a forecast model for active and reactive power and electricity price for future times, where the forecast is updated after each time step. We develop the forecasting model for net load with solar generation using AutoRegressive Moving Average (ARMA) model and electricity price forecast using AutoRegressive Integrated Moving Average (ARIMA). The details of modeling are provided in the supplementary material. The forecast values are fed to a Model Predictive Control (MPC) scheme [41] to identity the optimal modes of operation of storage for the current time-instance. Any of the developed schemes from the previous section can be used for the optimization inside MPC. These steps (forecast and MPC) are repeated sequentially and highlighted in online Algorithm 1: `ForecastPlusMPC`.

Algorithm 1 `ForecastPlusMPC`

Global Inputs: $\eta_{\text{ch}}, \eta_{\text{dis}}, \delta_{\max}, \delta_{\min}, b_{\max}, b_{\min}, S_B^{\max}$, b_0
Inputs: $h, N, T, i = 0$
while $i < N$ **do**
  $i = i + 1$
  Forecast $\hat{P}, \hat{Q}$ from time step i to N using ARMA
  Forecast $\hat{p}_{elec}$ from time step i to N using ARIMA
  Co-optimize arbitrage and PFC using inputs $\hat{p}_{elec}, \hat{P}, \hat{Q}, h$, battery parameters
  Find out battery output: P_B and Q_B
  $b^{i^*} = b^{i-1} + [P_B(i)]^+ \eta_{\text{ch}} - [P_B(i)]^- / \eta_{\text{dis}}$
  Update $b_0 = b^{i^*}$
end while

V. Numerical Results

In this section, we demonstrate the performance of our proposed optimization formulations through numerical simulations with real data. As described in Section III, we consider multiple storage control policies in the presence of solar, as listed below.

- P_{arb}: Only arbitrage,
- P_{mr}: McCormick relaxation for arbitrage + PFC,
- P_{rh}: Receding horizon arbitrage + sequential PFC,
- P_{plt}: Arbitrage + penalized PFC,
- P_{plt}^{conv}: Arbitrage + penalized PFC+converter usage.

The price data for our simulations is taken from NYISO [42]. The load and generation data is taken from data collected at Madeira, Portugal. We use the following performance indexes to measure the performance of our simulations:

1) *Arbitrage Gains*: effectiveness in performing arbitrage
2) *Power Factor Correction:* is gauged using 3 indices, using a prescribed PF limit of 0.9: (i) *No. of PF violations* denoted as VLT, (ii) *Mean PF*, and (iii) *Minimum PF*.
3) Converter Usage Factor (CUF): measures usage as

$$\text{CUF} = \frac{1}{N} \sum_{i=1}^{N} \frac{\sqrt{(P_B^i)^2 + (Q_B^i)^2}}{S_B^{\max}} \tag{14}$$

As a benchmark for PFC indices, in Table II, we list the values over a representative day, for two nominal cases: (a)$NSNB$ (no solar with no battery), and (b)SNB (solar with no battery). It is evident that with addition of solar, the PF seen by the grid deteriorates with number of PF violations increasing by 200% and minimum PF reached decreasing by 80%.

TABLE II: Nominal Cases without Energy Storage for 1 day

Parameters	$NSNB$	SNB
No. of PF violations	8	25
mean PF	0.9735	0.9054
min PF	0.8201	0.1587

In order to rectify the PF and perform arbitrage we add inverter connected energy storage. In numerical results, we use four batteries with differing converter capacities for comparison. Their parameters are listed in Table III. For fixed battery capacity, we consider four different ramp rates, each of which is described as a ratio of battery capacity over ramp rate. For instance xC-yC ramp rate in Table III will require 1/x hours to fully charge and 1/y hours to fully discharge. By Eq. 2, the ramp rate also fixes the maximum power $P_B^{\max}$. We define maximum converter capacity $S_B^{\max}$ in terms of $P_B^{\max}$. We consider 4 different battery converters: (i) $S_B^{\max} = P_B^{\max}$, (ii) $S_B^{\max} = 0.9P_B^{\max}$, (iii) $S_B^{\max} = 1.25P_B^{\max}$, (iv) $S_B^{\max} = 1.5P_B^{\max}$. The sampling time h is 15 minutes, time horizon T is 24 hours and the power factor limit set is 0.9.

TABLE III: Battery Parameters

$B_{\min}$, $B_{\max}$, B_0	200Wh, 2000 Wh, 1000 Wh
$\eta_{\text{ch}} = \eta_{\text{dis}}$	0.95
$\delta_{\max} = -\delta_{\min}$	500 W for 0.25C-0.25C, 1000 W for 0.5C-0.5C 2000 W for 1C-1C, 4000 W for 2C-2C

TABLE IV: Comparison of arbitrage gains for 1 day

Converter	Battery	P_{arb}	P_{mr}	P_{rh}	P_{plt}	P_{plt}^{conv}
$P_B^{\max}$	0.25C-0.25C	**0.1754**	N.F.	N.F.	0.1747	0.1747
	0.5C-0.5C	**0.2564**	0.2564	0.2564	0.2564	0.2564
	1C-1C	**0.3367**	0.3367	0.3367	0.3367	0.3367
	2C-2C	**0.4144**	0.4144	0.4144	0.4144	0.4144
$0.9P_B^{\max}$	0.25C-0.25C	**0.1728**	N.F.	N.F.	0.1704	0.1704
	0.5C-0.5C	**0.2523**	0.2511	0.2511	0.2511	0.2511
	1C-1C	**0.3314**	0.3314	0.3314	0.3314	0.3314
	2C-2C	**0.4098**	0.4098	0.4097	0.4098	0.4098
$1.25\times P_B^{\max}$	0.25C-0.25C	**0.1754**	N.F.	N.F.	0.1753	0.1753
	0.5C-0.5C	**0.2564**	0.2564	0.2564	0.2564	0.2564
	1C-1C	**0.3367**	0.3367	0.3367	0.3367	0.3367
	2C-2C	**0.4144**	0.4144	0.4144	0.4144	0.4144
$1.5P_B^{\max}$	0.25C-0.25C	**0.1754**	0.1754	0.1754	0.1754	0.1754
	0.5C-0.5C	**0.2564**	0.2564	0.2564	0.2564	0.2564
	1C-1C	**0.3367**	0.3367	0.3367	0.3367	0.3367
	2C-2C	**0.4144**	0.4144	0.4144	0.4144	0.4144

We compare the arbitrage gains in Table IV and PF violations in Table V respectively for different algorithms and battery settings over a day (96 time instances). Note the arbitrage gains with PFC matches with arbitrage gains for P_{arb}, implying performing PFC does not deteriorated energy storage's ability to perform arbitrage. For PF violations, as expected, the no. of PF violations for P_{arb} remain close to SNB. P_{mr} and P_{rh} are not feasible (denoted as N.F. in results) for battery with slowest ramp rate and small converter, i.e., PF violations are unavoidable. However, the other schemes are able to reduce the number of violations drastically. In settings where feasible solution exist, all schemes considered are able to completely avoid any violation. Table VI presents the mean PF. Note that for P_{mr} and P_{rh} in particular, the mean PF for a large converter approaches close to 1, which demonstrates their ability in PFC. However this may lead to overuse of the converter, as evident from CUF listed in Table VIII. Here P_{plt}^{conv} provides a way to balance CUF with mean PF as evident from both the tables. Table VII lists the minimum PF measured over the same day which is greater or equal to the threshold for feasible cases. However, further analysis would be required to determine penalty functions that motivate or hinder converter usage.

TABLE V: Comparison of no. of PF violations for 1 day

Converter	Battery	P_{arb}	P_{mr}	P_{rh}	P_{plt}	P_{plt}^{conv}
$P_B^{\max}$	0.25C-0.25C	27	N.F.	N.F.	2	2
	0.5C-0.5C	27	0	0	0	0
	1C-1C	26	0	0	0	0
	2C-2C	24	0	0	0	0
$0.9P_B^{\max}$	0.25C-0.25C	26	N.F.	N.F.	4	4
	0.5C-0.5C	23	0	0	0	0
	1C-1C	25	0	0	0	0
	2C-2C	24	0	0	0	0
$1.25\times P_B^{\max}$	0.25C-0.25C	26	N.F.	N.F.	1	1
	0.5C-0.5C	25	0	0	0	0
	1C-1C	26	0	0	0	0
	2C-2C	25	0	0	0	0
$1.5P_B^{\max}$	0.25C-0.25C	26	0	0	0	0
	0.5C-0.5C	25	0	0	0	0
	1C-1C	26	0	0	0	0
	2C-2C	25	0	0	0	0

TABLE VI: Comparison of mean PF for 1 day

Converter	Battery	P_{arb}	P_{mr}	P_{rh}	P_{plt}	P_{plt}^{conv}
$P_B^{\max}$	0.25C-0.25C	0.9062	N.F.	N.F.	0.9581	0.9562
	0.5C-0.5C	0.8803	0.9571	0.9850	0.9616	0.9567
	1C-1C	0.9077	0.9615	0.9938	0.9426	0.9602
	2C-2C	0.8997	0.9656	0.9983	0.9378	0.9638
$0.9P_B^{\max}$	0.25C-0.25C	0.9058	N.F.	N.F.	0.9512	0.9554
	0.5C-0.5C	0.8837	0.9580	0.9772	0.9661	0.9580
	1C-1C	0.9080	0.9610	0.9909	0.9560	0.9603
	2C-2C	0.9012	0.9659	0.9972	0.9648	0.9642
$1.25\times P_B^{\max}$	0.25C-0.25C	0.9062	N.F.	N.F.	0.9545	0.9567
	0.5C-0.5C	0.8803	0.9973	0.9903	0.9802	0.9802
	1C-1C	0.9077	0.9998	0.9962	0.9742	0.9742
	2C-2C	0.8997	0.9999	0.9987	0.9478	0.9478
$1.5P_B^{\max}$	0.25C-0.25C	0.9062	0.9934	0.9821	0.9850	0.9571
	0.5C-0.5C	0.8803	0.9987	0.9927	0.9832	0.9567
	1C-1C	0.9080	0.9999	0.9971	0.9839	0.9602
	2C-2C	0.8997	0.9999	0.9991	0.9244	0.9381

TABLE VII: Comparison of minimum PF for 1 day

Converter	Battery	P_{arb}	P_{mr}	P_{rh}	P_{plt}	P_{plt}^{conv}
$P_B^{\max}$	0.25C-0.25C	0.1587	N.F.	N.F.	0.8443	0.8443
	0.5C-0.5C	0.0321	0.9000	0.9000	0.9000	0.9000
	1C-1C	0.1587	0.9000	0.9568	0.9000	0.9000
	2C-2C	0.0545	0.9000	0.9821	0.9000	0.9000
$0.9P_B^{\max}$	0.25C-0.25C	0.1587	N.F.	N.F.	0.8295	0.8295
	0.5C-0.5C	0.0321	0.9000	0.9000	0.9000	0.9000
	1C-1C	0.1587	0.9000	0.9000	0.9000	0.9000
	2C-2C	0.0545	0.9000	0.9000	0.9000	0.9000
$1.25\times P_B^{\max}$	0.25C-0.25C	0.1587	N.F.	N.F.	0.8789	0.8789
	0.5C-0.5C	0.0321	0.9501	0.9303	0.9323	0.9000
	1C-1C	0.1587	0.9935	0.9681	0.9604	0.9000
	2C-2C	0.0545	0.9970	0.9842	0.9266	0.9000
$1.5P_B^{\max}$	0.25C-0.25C	0.1587	0.9015	0.9005	0.9000	0.9000
	0.5C-0.5C	0.0321	0.9739	0.9444	0.9638	0.9000
	1C-1C	0.1587	0.9935	0.9749	0.9765	0.9000
	2C-2C	0.0545	0.9993	0.9863	0.9124	0.9237

TABLE VIII: Comparison of CUF for 1 day

Converter	Battery	P_{arb}	P_{mr}	P_{rh}	P_{plt}	P_{plt}^{conv}
$P_B^{\max}$	0.25C-0.25C	0.7154	N.F.	N.F.	0.9198	**0.7390**
	0.5C-0.5C	0.6056	0.6246	0.6387	0.6789	**0.6230**
	1C-1C	0.5520	0.5611	0.5709	0.6011	**0.5568**
	2C-2C	0.4970	0.5048	0.5059	0.5248	**0.4985**
$0.9P_B^{\max}$	0.25C-0.25C	0.7693	N.F.	N.F.	0.9386	**0.7823**
	0.5C-0.5C	0.6373	0.6552	0.6694	0.7088	**0.6541**
	1C-1C	0.5787	0.5876	0.5989	0.6183	**0.5842**
	2C-2C	0.5284	0.5375	0.5398	0.5395	**0.5302**
$1.25\times P_B^{\max}$	0.25C-0.25C	0.5723	N.F.	N.F.	0.8045	**0.5992**
	0.5C-0.5C	0.4845	0.5605	0.5180	0.5513	**0.4984**
	1C-1C	0.4416	0.4796	0.4595	0.4648	**0.4454**
	2C-2C	0.3976	0.4106	0.4058	0.4208	**0.3988**
$1.5P_B^{\max}$	0.25C-0.25C	0.4770	0.5972	0.5277	0.6159	**0.5023**
	0.5C-0.5C	0.4037	0.4811	0.4379	0.4705	**0.4153**
	1C-1C	0.3680	0.4032	0.3844	0.4444	**0.3712**
	2C-2C	0.3311	0.3418	0.3387	0.3630	**0.3519**

It is clear from the mentioned results that storage devices over multiple settings can be used for PFC without any noticeable loss in arbitrage gains.

Fig. 5 presents the relationship between the PF threshold, mean PF and arbitrage gains for 1C-1C battery. As the effect of PF limit on the maximum possible arbitrage gains is almost non-existent except for PF limit close to 1. This resonates with our claim that PFC and arbitrage are largely decoupled and performing PFC do not degrade energy storage's ability to perform arbitrage. From Fig. 5 we also observe that the mean PF during the day when solar generation is available drops to 0.81 significantly lower than the mean PF for the whole day in absence of solar generation which is 0.97. Next, we discuss results of our developed algorithms in the setting with uncertain knowledge of future variables.

A. Results with uncertainty

In Section VI we propose a real-time implementation for performing PFC with arbitrage under uncertainty. The forecast

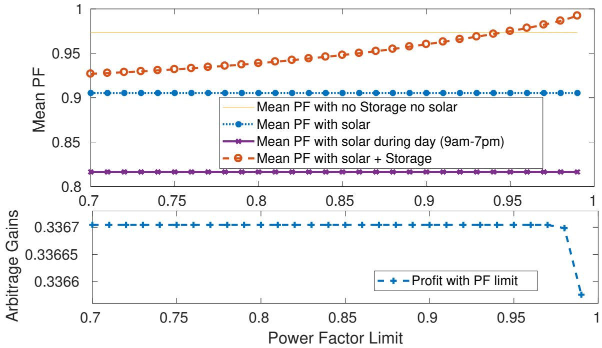

Fig. 5: Arbitrage gains and mean PF with varying PF limit for 1C-1C

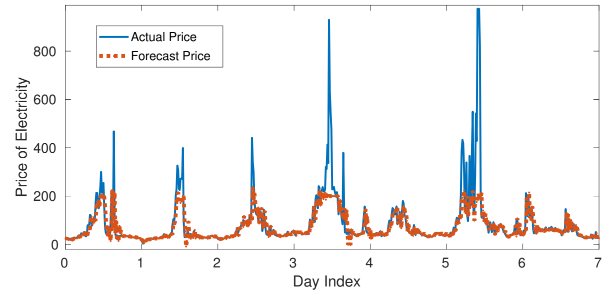

Fig. 7: ARIMA Price Forecast

model is generated for load with solar generation and for electricity price. The ARMA based forecast use 9 weeks of data for training and generates forecast for the next week. `ForecastPlusMPC` is implemented in receding horizon. The training data for net load seen by the grid with and without PV is plotted in Fig. 6. Fig. 6 indicate that inclusion of solar PV have degraded the PF significantly.

The performance of forecast of electricity price signal is plotted in Fig. 7. The electricity price data used for this numerical experiment is taken from CAISO for the same days of load data. Note that the ARIMA model for price misses peaks beyond \$200/MW. However, this drawback of the forecast model is not dominant for batteries with slow ramp rates as for such batteries the optimal control action for any price above \$200/MW is discharge the battery at maximum rate. Note \$200/MW is significantly higher than the mean electricity price. To compare the effect of forecasting

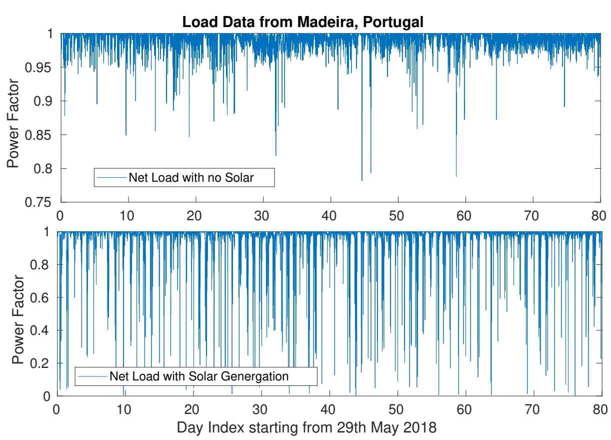

Fig. 6: Variation of PF with and without solar PV

net load and electricity prices with perfect information, we present average arbitrage gains and PFC indices for one week starting from 1st June 2018 using (P_{plt}) as the optimization scheme inside PFC. Table IX includes the deterministic results, while Table X includes the performance with uncertainty. Note that the arbitrage gain is more sensitive to uncertainty for fast ramping battery. This observation is in sync with [43]. PFC generally requires no-look-ahead as evident from comparison of (P_{mr}) and (P_{rh}). Note in Tables IX and X that future uncertainty does not affect the power factor violations significantly. It is however true that an undersized converter for slow ramping battery have a high CUF compared to other cases.

TABLE IX: Deterministic Performance

Converter	Battery	Gains	Mean PF	VLT	CUF	Min PF
$P_B^{\max}$	0.25C-0.25C	3.0645	0.9705	11	0.8972	0.0487
	0.5C-0.5C	4.7840	0.9713	2	0.7508	0.6665
	1C-1C	7.0592	0.9433	0	0.6924	0.9000
	2C-2C	9.4113	0.9364	0	0.5868	0.9000
$0.9P_B^{\max}$	0.25C-0.25C	3.0385	0.9644	26	0.9278	0.0883
	0.5C-0.5C	4.7251	0.9618	19	0.7951	0.2141
	1C-1C	6.9569	0.9663	2	0.7128	0.6330
	2C-2C	9.3096	0.9754	1	0.6149	0.5688
$1.25\times P_B^{\max}$	0.25C-0.25C	3.0647	0.9831	0	0.6985	0.9033
	0.5C-0.5C	4.7840	0.9799	0	0.6236	0.9352
	1C-1C	7.0593	0.9764	0	0.5495	0.9000
	2C-2C	9.4113	0.9769	0	0.4645	0.9000
$1.5P_B^{\max}$	0.25C-0.25C	3.0647	0.9803	0	0.6119	0.9000
	0.5C-0.5C	4.7840	0.9773	0	0.5267	0.9000
	1C-1C	7.0593	0.9762	0	0.4624	0.9000
	2C-2C	9.4113	0.9776	0	0.3874	0.9000

TABLE X: Performance with uncertainty model and MPC

Converter	Battery	Gains	Mean PF	VLT	CUF	Min PF
$P_B^{\max}$	0.25C-0.25C	2.9996	0.9704	13	0.9075	0.0488
	0.5C-0.5C	3.4962	0.9692	2	0.7746	0.6665
	1C-1C	4.6840	0.9465	0	0.7032	0.9000
	2C-2C	6.0345	0.9375	0	0.6142	0.9000
$0.9P_B^{\max}$	0.25C-0.25C	2.9718	0.9652	25	0.9324	0.0656
	0.5C-0.5C	3.3975	0.9630	21	0.8198	0.2152
	1C-1C	4.5934	0.9684	4	0.7258	0.6268
	2C-2C	5.9686	0.9771	1	0.6402	0.5762
$1.25\times P_B^{\max}$	0.25C-0.25C	2.9997	0.9827	0	0.7166	0.9000
	0.5C-0.5C	3.4962	0.9796	0	0.6493	0.9146
	1C-1C	4.6841	0.9763	0	0.5680	0.9122
	2C-2C	6.0345	0.9765	0	0.4889	0.9083
$1.5P_B^{\max}$	0.25C-0.25C	2.9997	0.9789	0	0.6220	0.9248
	0.5C-0.5C	3.4962	0.9774	0	0.5540	0.9105
	1C-1C	4.6841	0.9747	0	0.4768	0.9058
	2C-2C	6.0345	0.9778	0	0.4071	0.9103

VI. Conclusion

In this paper, we propose optimization formulations to operate inverter connected storage devices in distribution grids for co-optimizing arbitrage and power factor correction (PFC), both with or without perfect information. For a majority of cases, we show that the arbitrage gains with PFC converge to the gains achieved when storage performs only arbitrage. The primary reason for PFC being decoupled from arbitrage gains is due to the fact that in most instances, PF can be corrected by adjusting reactive power output. This is primarily governed by converter size and unlike storage active power output, which is constrained by capacity and ramp constraint. We also observe that arbitrage gain of batteries with higher ratio of ramp rate over capacity are more sensitive to uncertainty about future variables as they face capacity constraints more frequently.

It is also noteworthy that increasing the converter size would improve the mean PF without any significant change in arbitrage gains for the same ramping battery. In the current work, we consider a stringent case of maintaining PF for every operational point, though the methodology can be extended to the case with penalties on average PF. Moreover, in future work we will research further selection of optimal converter sizes and use solar and storage converter simultaneously. Finally we will also research directions to incorporate network power flow constraints pertaining to flow and voltage limits [44] into our work on energy storage.

REFERENCES

[1] C. A. Hill, M. C. Such, D. Chen, J. Gonzalez, and W. M. Grady, "Battery energy storage for enabling integration of distributed solar power generation," *IEEE Transactions on smart grid*, vol. 3, no. 2, pp. 850–857, 2012.

[2] J. Smith, W. Sunderman, R. Dugan, and B. Seal, "Smart inverter volt/var control functions for high penetration of pv on distribution systems," in *Power Systems Conference and Exposition (PSCE), 2011 IEEE/PES*. IEEE, 2011, pp. 1–6.

[3] M. Zuercher-Martinson, "Smart pv inverter benefits for utilities," *Renewable Energy World*, 2012.

[4] M. Kabir, Y. Mishra, G. Ledwich, Z. Y. Dong, and K. P. Wong, "Coordinated control of grid-connected photovoltaic reactive power and battery energy storage systems to improve the voltage profile of a residential distribution feeder." *IEEE Trans. Industrial Informatics*, vol. 10, no. 2, pp. 967–977, 2014.

[5] Energy efficiency improvement through optimization of the power factor correction. [Online]. Available: http://www2.schneider-electric.com/documents/technical-publications/en/shared/electrical-engineering/technical-papers/medium-voltage/energy_efficiency_CIRED_2007.pdf

[6] Power Factor Correction Enerdis France. [Online]. Available: http://www.enerdis.com/sites/default/files/documents/guide_compensation_906211239_bd.pdf

[7] J. Peronnet. Power factor correction kvar policy in countries. [Online]. Available: https://tinyurl.com/y437cpyd

[8] PLIEGO TARIFARIO, Gerencia Anlisis Tarifario, UTE Uruguay. [Online]. Available: http://tinyurl.com/y5ug28jh

[9] T. Stetz. German Guidelines and Laws for PV Grid Integration. [Online]. Available: https://tinyurl.com/yyc7dkcw

[10] Power factor design and reactive power capabilities - PJM ISO. [Online]. Available: https://tinyurl.com/yyv6ddv2

[11] Rule 21: Pacific Gas and Electric. [Online]. Available: https://www.pge.com/tariffs/tm2/pdf/ELEC_RULES_21.pdf

[12] Rule 21: Southern California Edison. [Online]. Available: https://www1.sce.com/NR/sc3/tm2/pdf/Rule21_1.pdf

[13] Rule 21: San Diego Gas & Electric. [Online]. Available: http://regarchive.sdge.com/tm2/pdf/ELEC_ELEC-RULES_ERULE21.pdf

[14] Pacific Gas and Electric Company Electric Tariff. [Online]. Available: https://www.pge.com/tariffs/tm2/pdf/ELEC_4795-E.pdf

[15] J. Matevosyan. ERCOT Renewable Integration. [Online]. Available: https://tinyurl.com/y5bss7zx

[16] FirstEnergy Corp: Customer Guide for Electric Service Ohio, 2017. [Online]. Available: https://tinyurl.com/y29gottk

[17] Hydro Ottawa Ltd: Conditions of Service 2017. [Online]. Available: https://tinyurl.com/y29bx85u

[18] Horizon 2020 Project Smile Deliverable 4.1, 2018. [Online]. Available: http://tinyurl.com/y4285y49

[19] Linky Single-Phase Smart Meters. [Online]. Available: https://www.enedis.fr/sites/default/files/Notice_compteur_Linky_Monophase_anglais.pdf

[21] H. Ren, Q. Wu, W. Gao, and W. Zhou, "Optimal operation of a grid-connected hybrid pv/fuel cell/battery energy system for residential applications," *Energy*, vol. 113, pp. 702–712, 2016.

[20] Power Factor Correction (PFC) in solar power plants. [Online]. Available: https://tinyurl.com/y3njurn4

[22] M. Hashmi, A. Mukhopadhyay, A. Busic, and J. Elias, "Storage optimal control under net metering policies," *to be submitted IEEE Transactions on Smart Grid*, 2018.

[23] S. Karagiannopoulos, P. Aristidou, and G. Hug, "Hybrid approach for planning and operating active distribution grids," *IET Generation, Transmission & Distribution*, vol. 11, no. 3, pp. 685–695, 2017.

[24] B. Singh, K. Al-Haddad, and A. Chandra, "A review of active filters for power quality improvement," *IEEE transactions on industrial electronics*, vol. 46, no. 5, pp. 960–971, 1999.

[25] B. Kirby, O. Ma, and M. O'Malley, "The value of energy storage for grid applications," *National Renewable Energy Laboratory. May. http://www.nrel. gov/docs/fy13osti/58465. pdf (accessed October 21, 2014)*, 2013.

[26] A. Ellis, R. Nelson, E. Von Engeln, R. Walling, J. MacDowell, L. Casey, E. Seymour, W. Peter, C. Barker, B. Kirby *et al.*, "Review of existing reactive power requirements for variable generation," in *Power and Energy Society General Meeting, 2012 IEEE*. IEEE, 2012, pp. 1–7.

[27] K. Turitsyn, P. Sulc, S. Backhaus, and M. Chertkov, "Local control of reactive power by distributed photovoltaic generators," in *Smart Grid Communications (SmartGridComm), 2010 First IEEE International Conference on*. IEEE, 2010, pp. 79–84.

[28] M. Alam, K. Muttaqi, and D. Sutanto, "Distributed energy storage for mitigation of voltage-rise impact caused by rooftop solar pv," in *Power and Energy Society General Meeting, IEEE*. IEEE, 2012, pp. 1–8.

[29] E. Muljadi, C. Butterfield, R. Yinger, and H. Romanowitz, "Energy storage and reactive power compensator in a large wind farm," in *42nd AIAA Aerospace Sciences Meeting and Exhibit*, 2004, p. 352.

[30] Z. Taylor, H. Akhavan-Hejazi, and H. Mohsenian-Rad, "Power hardware-in-loop simulation of grid-connected battery systems with reactive power control capability," in *Power Symposium (NAPS), 2017 North American*. IEEE, 2017, pp. 1–6.

[31] B. Cheng and W. Powell, "Co-optimizing battery storage for the frequency regulation and energy arbitrage using multi-scale dynamic programming," *IEEE Transactions on Smart Grid*, pp. 1–1, 2016.

[32] Y. Shi, B. Xu, D. Wang, and B. Zhang, "Using battery storage for peak shaving and frequency regulation: Joint optimization for superlinear gains," *IEEE Transactions on Power Systems*, vol. 33, no. 3, pp. 2882–2894, 2018.

[33] "Battery Energy Storage System: The power to control energy by Ved Sinha (ABB)." [Online]. Available: https://tinyurl.com/y9qle48y

[34] M. C. Kisacikoglu, B. Ozpineci, and L. M. Tolbert, "Reactive power operation analysis of a single-phase ev/phev bidirectional battery charger," in *Power Electronics and ECCE Asia (ICPE & ECCE), 2011 IEEE 8th International Conference on*. IEEE, 2011, pp. 585–592.

[35] M. Hashmi, A. Mukhopadhyay, A. Busic, and J. Elias, "Optimal control of storage under time varying electricity prices," in *IEEE International Conference on Smart Grid Communications*, 2017.

[36] McCormick envelopes. [Online]. Available: https://optimization.mccormick.northwestern.edu/index.php/McCormick_envelopes

[37] G. P. McCormick, "Computability of global solutions to factorable nonconvex programs: Part iconvex underestimating problems," *Mathematical programming*, vol. 10, no. 1, pp. 147–175, 1976.

[38] H. Nagarajan, M. Lu, E. Yamangil, and R. Bent, "Tightening mccormick relaxations for nonlinear programs via dynamic multivariate partitioning," in *International Conference on Principles and Practice of Constraint Programming*. Springer, 2016, pp. 369–387.

[39] CVX: Matlab Software for Disciplined Convex Programming, version 2.0. [Online]. Available: http://cvxr.com/cvx

[40] S. Yang, D. Xiang, A. Bryant, P. Mawby, L. Ran, and P. Tavner, "Condition monitoring for device reliability in power electronic converters: A review," *IEEE Transactions on Power Electronics*, vol. 25, no. 11, pp. 2734–2752, 2010.

[41] E. F. Camacho and C. B. Alba, *Model predictive control*. Springer Science & Business Media, 2013.

[42] "Real Time LMP, New York ISO." [Online]. Available: https://tinyurl.com/2flowo6

[43] Y. Chen, M. U. Hashmi, D. Deka, and M. Chertkov, "Stochastic battery operations using deep neural networks," in *IEEE ISGT, NA*, 2019.

[44] A. Hassan, R. Mieth, M. Chertkov, D. Deka, and Y. Dvorkin, "Optimal load ensemble control in chance-constrained optimal power flow," *IEEE Transactions on Smart Grid*, pp. 1–1, 2018.